

INTERACTION OF VENTILATING JETS

by

ARNALDO MARANGONI

Engenheiro de Aeronautica-Aeronaves  
Brazilian Aeronautical Institute of  
Technology, 1963

---

A MASTER'S THESIS

submitted in partial fulfillment of the  
requirements for the degree

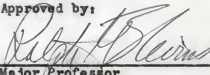
MASTER OF SCIENCE

Department of Mechanical Engineering

KANSAS STATE UNIVERSITY  
Manhattan, Kansas

1966

Approved by:

  
\_\_\_\_\_  
Major Professor

LD  
2668  
T4  
1966  
m311  
c.2

## TABLE OF CONTENTS

NOMENCLATURE .....	1
INTRODUCTION .....	1
JET CHARACTERISTICS .....	1
MOMENTUM EQUATION FOR A SINGLE JET AT THE SAME TEMPERATURE OF THE SURROUNDING AIR AT REST .....	2
THE CENTER LINE VELOCITY DISTRIBUTION FOR A SINGLE JET AT THE SAME TEMPERATURE OF THE SURROUNDING AIR AT REST .....	6
MOMENTUM EQUATION FOR A SINGLE JET AT LOWER TEMPERATURE THAN THE SURROUNDING AIR AT REST .....	8
COMPARISON BETWEEN THE ORDER OF MAGNITUDE OF THE INERTIAL FORCES, BUOYANCY FORCES AND SHEARING FORCES IN TURBULENT JET FLOW .....	12
DISTANCE FROM THE OUTLET WHERE AN EQUALIZATION OF VELOCITIES MAY BE EXPECTED .....	13
DESCRIPTION OF THE APPARATUS .....	14
EXPERIMENTAL DATA .....	15
RESULTS .....	15
CONCLUSIONS .....	16
ACKNOWLEDGEMENT .....	18
REFERENCES .....	19
APPENDIX .....	20

# NOMENCLATURE

$b$	Distance from the x-axis where the velocity may be considered as being practically zero, ft
$d$	Diameter of the hole from where the jet escapes, ft
$e$	Constant, ft
$l$	Mixing length, ft
$g$	Gravitational acceleration, ft/sec <sup>2</sup>
$M_0$	Rate of momentum evaluated at the jet outlet, lb <sub>f</sub>
$r$	Distance measured from the x-axis and at right angles to it, ft
$\bar{T}$	Mean temperature, °R
$T_0$	Surrounding temperature, °R
$u_0$	Jet outlet velocity, ft/sec
$u_{max}$	Maximum value of the mean velocity attained at $r = 0$ , ft/sec
$\bar{u}$ and $\bar{v}$	Components of the mean velocity in the directions of x and r, respectively, ft/sec
$u'$ and $v'$	Components of the fluctuating velocity in the x- and r- directions respectively, ft/sec
$x$	Distance from the jet outlet measured along the axis of the jet, ft
$\tau$	Shearing stress, lb <sub>f</sub> /sqft
$\rho$	Density, lb <sub>f</sub> .sec <sup>2</sup> /ft <sup>4</sup>
$\nu$	Viscosity, ft <sup>2</sup> /sec

## Dimensionless groups

$Re$	Reynold's number, $u_0 \cdot d / \nu$
$\eta$	Dimensionless parameter, $r/b$
$\alpha$ $\beta$	Proportionality constants
$c$	Constant

## INTRODUCTION

The jet flow from an opening at sufficiently high value of Reynold's number is characterized by a turbulent phenomenon known as free turbulence. To explain this phenomena several theories have been developed. Basically, in these theories the turbulent phenomena is studied according to the " Statistical Theory of Turbulence "<sup>1</sup> or according to " Prandtl's mixing length theory "<sup>2</sup>.

The problem of a single turbulent jet mixing of incompressible fluid was first analysed successfully by Tollmien<sup>3</sup>. In his theoretical analysis Tollmien used the Prandtl's mixing length theory<sup>4</sup>.

It appears feasible to apply the mixing length theory to the study of the interaction of ventilating jets because Tollmien's theoretical analysis using the mixing length theory, agreed fairly well with experimental results.

The purpose of the present work is to determine the points of interaction of parallel axially symmetric jets escaping from three 1/4 inch diameter holes spaced one inch apart and to determine the distance from the jet outlet for equalization of velocities.

These investigations were made using smoke photographs of the jets and measurements of the jet velocities with a No. 18 hypodermic needle as an impact tube and with a heated thermocouple anemometer.

## JET CHARACTERISTICS

There are three regions in the jet (Fig. 1a): region I, there is a potential core in the central part of the jet and a mixing zone; region II, where there is a transition zone and region III where there is fully developed flow.

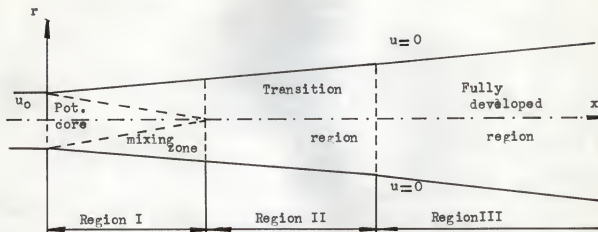


Fig. 1a

The length of region I extends about 4 diameters from the nozzle<sup>5</sup> and the fully developed region is achieved at about 10 diameters downstream<sup>6</sup>.

It is known also that the velocity profile in the fully developed region follows an exponential law<sup>7</sup> given by:

$$\frac{\bar{u}}{u_{\max}} = \exp \left[ -k(r/x)^2 \right] \quad (1)$$

where  $k$  is an exponential experimental constant. This velocity distribution was assumed and then verified experimentally. It may be also calculated from the differential equation of the motion<sup>8</sup>.

#### MOMENTUM EQUATION FOR A SINGLE JET AT THE SAME TEMPERATURE OF THE SURROUNDING AIR AT REST

Referring to Fig. 1b

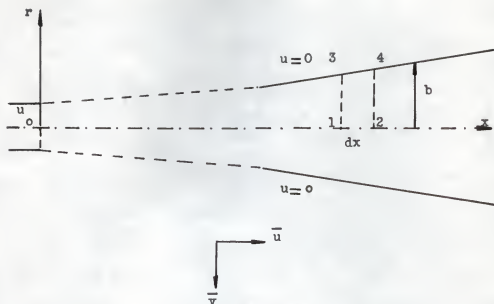


Fig. 1b

Assuming that the jet has a definite breadth  $b$ , that is, a distance from the  $x$ -axis where the velocity may be considered as being practically zero. Then the mass flow rate across 1-3 is equal to

$$\int_0^b 2\pi\rho\bar{u}rdr$$

where the bar refers to the mean value. The mass flow rate across 2-4 is

$$\int_0^b 2\pi\rho\bar{u}rdr + \frac{d}{dx} \left[ \int_0^b 2\pi\rho\bar{u}rdr \right] dx$$

Thus the mass flow rate across 2-4 exceeds that across 1-3 by

$$\frac{d}{dx} \left[ \int_0^b 2\pi\rho\bar{u}rdr \right] dx$$

and this must be the inward mass flow rate across 3-4. The fluid crossing 3-4 is assumed to be at zero velocity and thus the inward flux of momentum across 3-4 is zero.

The influx of momentum across 1-3 is

$$\int_0^b 2\pi \rho \bar{u}^2 r dr$$

and the out flux of momentum across 2-4 is

$$\int_0^b 2\pi \rho \bar{u}^2 r dr + \frac{d}{dx} \left[ \int_0^b 2\pi \rho \bar{u}^2 r dr \right] dx.$$

Thus, the flux of momentum across 2-4 exceeds that across 1-3 by

$$\frac{d}{dx} \left[ \int_0^b 2\pi \rho \bar{u}^2 r dr \right] dx.$$

The forces acting on the fluid in the x-direction are the shearing stress and the force due to the difference of pressures on 1-3 and 2-4. Neglecting the viscous stresses, the shearing stress,  $\gamma$ , at any point in the fluid is given by

$$\gamma = -\rho \overline{u'v'}$$

where the prime refers to turbulent fluctuations. The pressure difference is

usually considered negligible. Thus, the rate at which momentum is convected in the x-axis direction is

$$\frac{d}{dx} \int_0^b 2\pi \rho \bar{u}^2 r dr = (\tau)_0^b \quad (2)$$

It should be observed that the term due to the mass flow rate

$$\frac{d}{dx} \left[ \int_0^b 2\pi \rho \bar{u}^2 r dr \right] dx$$

does not appear in the equation (2) because it was considered that the velocity  $u=0$  at  $r=b$ .

Considering the fluid properties being constants, equation (2) reduces to

$$2\pi \rho \frac{d}{dx} \int_0^b \frac{1}{2} \bar{u}^2 r dr = 0 \quad (3)$$

since the shearing stress is zero at  $r=0$  and  $r=b$ .

Integration of (3) gives

$$2\pi \rho \int_0^b \frac{1}{2} \bar{u}^2 r dr = M_0 = \text{constant} \quad (4)$$



Equation (4) express that the momentum is constant along the x-axis.

THE CENTER LINE VELOCITY DISTRIBUTION FOR A SINGLE JET AT  
THE SAME TEMPERATURE OF THE SURROUNDING AIR AT REST

In the fully developed turbulent jet, the similarity of the velocity profile may be assumed and thus

$$\frac{\bar{u}}{u_{\max}} = f(\eta) \quad (5)$$

where  $\eta = r/b$  and  $u_{\max}$  - center line velocity.

Combining (4) and (5) and substituting the value of  $M_o$  from its value at the jet exit, then it can be shown

$$\frac{u_{\max}}{u_o} = \frac{1}{\sqrt{8I}} \cdot \frac{d}{b} \quad (6)$$

where

$$I = \int_0^1 f(\eta)^2 \eta d\eta$$

and

$$M_o = \rho u_o^2 \frac{\pi d^2}{4}$$

Prandtl assumed that in cases like the mixing of a free jet having a sufficiently high value of Reynold's number with the fluid at rest surrounding it, it is reasonable to take the mixing length,  $l$ , for every cross section as being proportional to the breadth of the jet there

$$l = \alpha b .$$

He then proved that the breadth is a linear function of  $x$

$$b = \beta x . \quad (7)$$

Pai and Schlichting using the same assumption of Prandtl, also proved, by using the substantial derivative method, that  $b$  is a linear function of  $x$  such that

$$b = cx + e \quad (8)$$

where  $c$  and  $e$  are constants. The constant term,  $e$ , which appears in the above equation can be made to vanish by a suitable choice of the origin of the coordinate system.

Combining equations (6) and (7)

$$\frac{u_{\max}}{u_0} = \frac{1}{\beta \sqrt{8I}} \frac{d}{dx} \quad (9)$$

Equation (9) shows that the center line velocity distribution obeys an hyperbolic law. From experimental results (Figs. 5 and 6) it can be seen that this law is fairly well approximated.

# MOMENTUM EQUATION FOR A SINGLE JET AT LOWER TEMPERATURE THAN THE SURROUNDING AIR AT REST

The momentum equation is similar to that derived in the previous section, except that it is necessary to add the term arising from the buoyancy forces. Using the same assumptions as for the previous case, equation (3) is then replaced by

$$2\pi\rho\frac{d}{dx}\int_0^b\bar{u}^2rdr=2g\pi\rho\int_0^b\frac{\bar{T}-T_0}{T_0}rdr$$

and

$$\frac{d}{dx}\int_0^b\bar{u}^2rdr=g\int_0^b\frac{\bar{T}-T_0}{T_0}rdr \quad (10)$$

Equation (10) shows that the velocity and temperature fields are interdependent and Equation (4) does not hold for this case because that in its derivation it was assumed that the jet and the surrounding were at same temperature.

## COMPARISON BETWEEN THE ORDER OF MAGNITUDE OF THE INERTIAL FORCES, BUOYANCY FORCES AND SHEARING FORCES IN TURBULENT JET FLOW

The equation of motion on the momentum transfer theory, with Prandtl's assumption for the mixing length, is

$$\bar{u} \frac{\partial \bar{u}}{\partial x} + v \frac{\partial \bar{u}}{\partial r} = - \frac{1}{r} \frac{\partial}{\partial r} \left[ l^2 r \left( \frac{\partial \bar{u}}{\partial r} \right)^2 \right] \quad (11)$$

for the case of non-cooled jet<sup>9</sup>, where

$$\gamma = -\rho l^2 \left( \frac{\partial \bar{u}}{\partial r} \right)^2 \quad (12)$$

the minus sign holds for positive values of  $r$ .

In order to compare the magnitude of the forces,  $\frac{\partial \bar{u}}{\partial r}$  is replaced by its approximated value

$$- \frac{2 u_{\max}}{b}$$

in expression (12)

$$\gamma_m = -4\rho l^2 \left( \frac{u_{\max}}{b} \right)^2 \quad (13)$$

According to Prandtl's assumption

$$l = \alpha b.$$

where

$$\alpha = 0.125 .$$

This value of  $\alpha$  is based on experimental results and is found in Ref. 2 .

Thus, equation (13) may be written

$$\gamma_m = -4\rho\alpha^2 u_{\max}^2 \quad (14)$$

as the mean value over the cross-section.

According to the equation of motion (11) the shear force per unit volume is

$$\frac{\partial \gamma}{\partial r}$$

starting from the middle of the jet,  $\gamma$  increases from zero to a maximum and then decreases to zero again, so that  $\frac{\partial \gamma}{\partial r}$  is first positive and then negative. For the central flow  $\frac{\partial \gamma}{\partial r}$  is taken as being proportional to

$$\frac{2\gamma_m}{b}$$

The buoyancy force per unit volume is

$$\varepsilon\rho \frac{\bar{T} - T_0}{T_0}$$

For the inertial force per unit volume, replace

$$u \frac{\partial u}{\partial x}$$

by its approximate value

$$\frac{u_{\max}^2}{x}$$

Now, in order to compare, let us take some practical values.

Suppose the case where

$$u_o = 108 \text{ fps}$$

and

$$x = 5''$$

$$d = 1/4''$$

then, from Fig. 5 and equation 8 <sup>7</sup>

$$u_{\max} = 27.5 \text{ fps}$$

and

$$b = 0.500''$$

Evaluating the inertial forces and the force due to the shearing stress based on these values it results

$$\frac{\text{inertial forces}}{\text{unit volume}} \sim \frac{\rho u_{\max}^2}{x} = \frac{\rho (27.5)^2 \cdot 12}{5} = 1815 \rho$$

and

$$\frac{\text{force due to shearing stress}}{\text{unit volume}} \sim \frac{2\gamma_m}{b} = \frac{-8\rho\alpha^2 u_{\max}^2}{b} = -2270\rho$$

Assuming also that the surrounding fluid is at  $80^\circ\text{F}$  and that  $\bar{T} - T_0 = 30^\circ\text{R}$ , it can be written for the buoyancy force per unit volume

$$\frac{\text{buoyancy force}}{\text{unit volume}} = \frac{\rho g(\bar{T} - T_0)}{T_0} = \frac{32.2(30\rho)}{540} = 1.79\rho$$

Hence the buoyancy force can be neglected compared to inertial and viscous forces as far as the application of jets in ventilation is concerned. Thus, from now on it may be assumed that the previous equations are valid for both cooled and non-cooled jets.

#### INTERACTION OF PARALLEL JETS HAVING THE SURROUNDINGS AT REST

Throughout the jets the pressure is nearly the same as in the surrounding air and considering that from each opening the air issues at the same velocity and in state steady, it may be assumed that the center lines of the jets are parallels and perpendicular to the plane of the outlet (Fig.2)

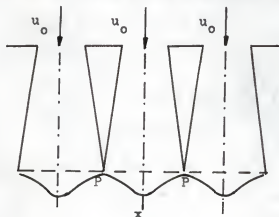


Fig. 2

Equation (8) may be used to calculate the interaction point P or may also be used to predict the spacing,  $s$ , among the jets.

DISTANCE FROM THE OUTLET WHERE AN EQUALIZATION OF VELOCITIES MAY BE EXPECTED

Since no satisfactory theory of turbulent flow presently exists, some simplifying assumptions were made pertaining to the nature of the interacting jets. It was assumed therefore that the velocity profiles could be superimposed as in Fig. 3

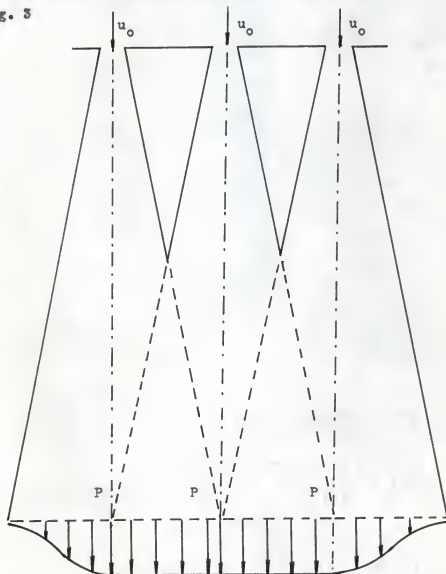


Fig. 3



Using equation (8) and considering that the breadth is equal to the spacing between the jets at the point P of equalization of velocity (Fig. 3), one may determine the distance,  $x$ , of the point P from the jet outlet. Then, equation (9) may be used to calculate the velocity of equalization.

The constants for equation (8) are determined from Figs. 7-11. Equation (9) is plotted in Figs. 5-6 for different outlets velocities.

#### DESCRIPTION OF THE APPARATUS

The air jet was directed downward from a plenum supplied by compressed air from an air compressor. The unit consisted of a plenum, flowmeter, pressure gage, smoke generator and a control valve. To obtain uniform flow of air through the orifices the plenum was provided with a wire screen. The plenum could be moved vertically to vary the height of the jet (Fig. 4)

Instrumentation. The pitot tube and the heated thermocouple anemometer could be moved vertically along the jet axis and transversally across the jet. The velocity was sensed by a No. 18 hypodermic needle employed as a total-head impact tube. The pressure was sensed with a micromanometer which had a nominal accuracy of  $\pm 0.001$  inch of water. For very low velocity measurements, the pitot tube was replaced by a heated thermocouple anemometer. The emf was measured with a millivolt potentiometer.

The smoke generator was used to provide a white jet which could be photographed. Sample photos are given in Figs. 12-16.

The control valve with feedback was used to prevent pressure oscillations in the plenum. The distance of the plenum from the moving platform was great enough in order to avoid recirculation of air.

## EXPERIMENTAL DATA

Center line velocities were measured for the case of a single hole at two different values of Reynold's number (Table I and II). These data are shown in Fig. 5 with a plot of equation 9. From this plot it is possible to determine experimentally the constant coefficient of that equation. These experimental results were then compared with the case when the air was issuing from three parallel holes (Table III, IV and V). Fig. 6 shows the plot of the data from Table III, IV and V and from this figure it is possible to determine the experimental coefficient of equation 9 for the case of three parallel jets.

In order to evaluate the constant terms of equation 8 a photographic method was used. Figs. 7-11 shows the projection of the jets issuing from the holes at different velocities. Figs. 12-16 are photographs corresponding to Figs. 7-11.

## RESULTS

## Comparison Between Measured and Theoretically Predicted Velocities

The comparison was carried out when using three holes at one inch spacing. The distance from the outlet at which the velocities are equalized may be calculated from equation (8), using the appropriate constants for a given outlet velocity. Knowing the distance,  $x_0$ , and using Fig. 6, the center line velocity at  $x_0$  (the velocity of equalization) can be calculated. The results for  $u_0 = 63.0, 76.7$  and  $91.6$  fps are given in Table VI and compared with measured values.

The deviation observed between the predicted and the measured values

may be attributed first to the fact that at a great distance from the outlet the hyperbolic law for the center line velocity deviates from the experimental data and secondly to the fact that when using the thermocouple anemometer the velocities measurements cannot be made at a point and this may induce errors in the measurements.

The second type of error may be avoided by carrying out velocity measurements in the central region of the interaction of 9 parallel jets spaced of 1 inch. The results for  $u_0 = 63.0$  and  $76.7$  fps are given in Table VII and compared with measured values.

#### CONCLUSIONS

I. Comparing the experimental results shown in Figs. 5 and 6, it can be seen that there is a slight modification of the constant term of equation 9 when measuring central line velocities from a single hole and when measuring velocities from the central hole of three holes. It was observed also that this deviation increases after the point where the velocities are equalized. However, even for a single jet, it was observed by previous investigators<sup>6</sup> that the velocity on the axis of the jet decreases, approximately following a hyperbolic power law for 10 to 30 diameters downstream, then deviating markedly at greater distances. In this investigation the point where equalization of velocities occurred at about 40 diameters from the outlet.

II. According to the measurements shown in Figs. 7-11, a slight increase in breadth by decreasing the outlet velocity is noted. However, a single equation cannot be given for the breadth at lower velocities because of the scatter of experimental measurements. By comparing Figs. 7 and 8 these deviations can be observed. Evidently, low velocities with turbulence are desirable not only

because of the increase in breadth but also because the effect of turbulent mixing tend to provide uniform temperature and velocity distributions throughout the space.

III. The following procedure must be followed to determine the location of the equalization of velocity and the velocity of equalization itself:

- a- Knowing the outlet velocity and the spacing between the jets the distance,  $x_e$ , can be determined from Fig. 17.
- b- Knowing the hole diameter and  $x_e$  the velocity of equalization can be determined from Fig. 6.

Note:  $x_e$  is the distance from the outlet of the jet where the velocity of equalization may be expected.

#### ACKNOWLEDGEMENT

The author wishes to express his gratitude to Dr. Ralph G. Nevins for his assistance in the writing and organisation of this thesis.

## REFERENCES

1. Taylor, G. I.  
Statistical theory of turbulence I-V, Proc. Roy. Soc.(London) A 151  
1935 and 1936.
- 2.\* Prandtl, Ludwig  
Essentials of fluid dynamics. Hafner Publishing Company, 1952, pp. 103-  
123.
- 3.\* Tollmien, Walter  
Berechnung der turbulenten Ausbreitungsvorgänge, ZAMM, 1926. Available  
as NACA TM 1085, 1945.
- 4.\* Pai, Shih-I  
Fluid dynamics of jets. D. Van Nostrand Company Inc., 1954, pp.99-116.
- 5.\* Kueths, A. M.  
Investigations of the turbulent mixing regions formed by jets. Journal  
Appl. Mech. 2, N<sup>o</sup> 3, September 1935.
- 6.\* Corrsin, S.  
Investigation of flow in an axially symmetric heated jet of air. NACA  
Wartime Report W-94, December 1943.
- 7.\* Albertson, M. L. and others  
Diffusion of submerged jets. Transactions, A.S.C.E. vol. 115, 1950, pp.  
650-685.
- 8.\* Schlichting, Hermann  
Boundary Layer Theory. McGraw-Hill Book Company, Inc. 1960, pp. 593-608.
- 9.\* Goldstein, Sidney  
Modern development in fluid dynamics. Oxford University Press, 1938 vol.  
II, p. 595.
- 10.\* Szablewski, W.  
Contributions to the theory of spreading of a free jet issuing from a  
nozzle. Available as NACA TM 1311.
- 11.\* Belander, Linn  
Characteristics of downward jets from a vertical discharge unit heater,  
ASHAE, November 1955.  
Outlet characteristics that affect the downward throw of heated air jets  
ASHAE journal, December 1956.  
Personal notes.

## APPENDIX

EXPLANATION OF PLATE I

Fig. 4. Schematic diagram of the unit used in  
present investigation.



## PLATE I

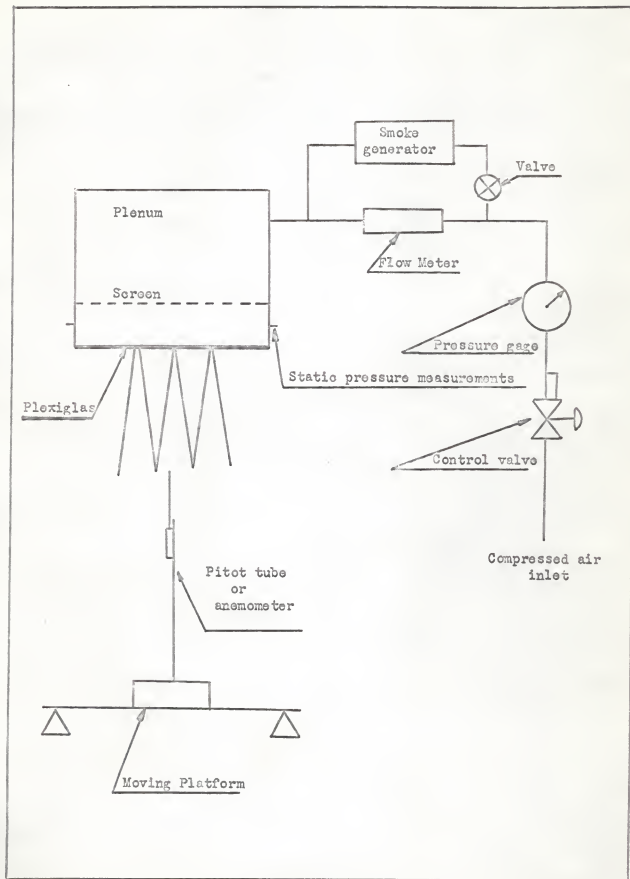


Fig. 4

EXPLANATION OF PLATE II

Table I. Distribution of the center line velocity for flow from a single jet. Air temperature 28° c and hole diameter 1/4".

## PLATE II

$x$ (in)	$u$ $\Delta h$ (in water)	$x/d$	$u_{\max}/u_0$
0.0	2.500	0.0	1.000
0.2	2.470	0.8	0.995
0.4	2.465	1.6	0.994
0.6	2.455	2.4	0.990
0.8	2.395	3.2	0.980
1.0	2.266	4.0	0.954
1.2	2.070	4.8	0.910
1.4	1.790	5.6	0.847
1.6	1.580	6.4	0.795
1.8	1.262	7.2	0.720
2.0	1.118	8.0	0.686
2.5	0.765	10.0	0.555
3.0	0.552	12.0	0.470
3.5	0.395	14.0	0.398
4.0	0.300	16.0	0.348
4.5	0.245	18.0	0.314
5.0	0.184	20.0	0.272
6.0	0.135	24.0	0.232
7.0	0.093	28.0	0.193
8.0	0.070	32.0	0.168
9.0	0.050	36.0	0.141
10.0	-	-	-

Table I

EXPLANATION OF PLATE III

Table II. Distribution of the center line velocity for flow from a single jet. Air temperature 25°C and hole diameter 1/4".

## PLATE III

$x$ (in)	$u$ $\Delta h$ (in water)	$x/d$	$u_{\max}/u_o$
0.0	15.450	0.0	1.000
0.2	15.400	0.8	1.000
0.4	15.350	1.6	0.995
0.6	15.300	2.4	0.994
0.8	15.100	3.2	0.990
1.0	14.300	4.0	0.964
1.2	12.500	4.8	0.903
1.4	11.200	5.6	0.853
1.6	9.610	6.4	0.789
1.8	8.390	7.2	0.736
2.0	7.160	8.0	0.680
2.5	4.620	10.0	0.548
3.0	3.200	12.0	0.456
3.5	2.880	14.0	0.432
4.0	1.770	16.0	0.340
4.5	1.385	18.0	0.300
5.0	1.070	20.0	0.264
6.0	0.715	24.0	0.215
7.0	0.520	28.0	0.183
8.0	0.280	32.0	0.134
9.0	0.280	36.0	0.134
10.0	0.240	40.0	0.125

Table II

EXPLANATION OF PLATE IV

Table III. Distribution of the center line velocity for flow from a central hole( 3 holes spaced 1" ). Air temperature 27°C and hole diameter 1/4".

## PLATE IV

$x$ (in)	$u$ $\Delta h$ (in water)	$x/d$	$u_{\max}/u_o$
0.0	0.800	0.0	1.000
0.2	0.800	0.8	1.000
0.4	0.800	1.6	1.000
0.6	0.800	2.4	1.000
0.8	0.751	3.2	0.970
1.0	0.595	4.0	0.865
1.2	0.560	4.8	0.840
1.4	0.427	5.6	0.732
1.6	0.348	6.4	0.660
1.8	0.305	7.2	0.620
2.0	0.260	8.0	0.570
2.5	0.170	10.0	0.462
3.0	0.130	12.0	0.405
3.5	0.093	14.0	0.340
4.0	0.070	16.0	0.296
4.5	0.060	18.0	0.274
5.0	0.040	20.0	0.224
6.0	0.029	24.0	0.191

Table III

#### EXPLANATION OF PLATE V

Table IV. Distribution of the center line velocity for flow from a central hole( 3 holes spaced 1" ). Air temperature 28° C and hole diameter 1/4".



PLATE V

$x$ (in)	$u$ $\Delta h(\text{in water})$	$x/d$	$u_{\text{max}}/u_o$
0.0	2.520	0.0	1.000
0.2	2.518	0.8	1.000
0.4	2.515	1.6	1.000
0.6	2.495	2.4	0.995
0.8	2.440	3.2	0.985
1.0	2.275	4.0	0.950
1.2	2.080	4.8	0.910
1.4	1.780	5.6	0.840
1.6	1.510	6.4	0.775
1.8	1.280	7.2	0.714
2.0	1.100	8.0	0.661
2.5	0.730	10.0	0.540
3.0	0.505	12.0	0.480
3.5	0.345	14.0	0.364
4.0	0.290	16.0	0.340
4.5	0.235	18.0	0.297
5.0	0.170	20.0	0.260
6.0	0.110	24.0	0.209
7.0	0.080	28.0	0.178
8.0	0.070	32.0	0.167
9.0	0.040	36.0	0.126
10.0	0.040	40.0	0.126

Table IV

EXPLANATION OF PLATE VI

Table V. Distribution of the center line velocity for flow from  
a central hole( 3 holes spaced 1" ). Air temperature  
28° C and hole diameter 1/4".

PLATE VI

$x$ (in)	$u$ $\Delta h(\text{in water})$	$x/d$	$u_{\max}/u_0$
0.0	9.595	0.0	1.000
0.2	9.580	0.8	1.000
0.4	9.575	1.6	1.000
0.6	9.420	2.4	0.994
0.8	9.230	3.2	0.982
1.0	8.890	4.0	0.965
1.2	8.210	4.8	0.925
1.4	7.175	5.6	0.866
1.6	5.820	6.4	0.780
1.8	4.690	7.2	0.700
2.0	4.020	8.0	0.650
2.5	2.750	10.0	0.540
3.0	1.880	12.0	0.443
3.5	1.350	14.0	0.376
4.0	1.010	16.0	0.325
4.5	0.770	18.0	0.284
5.0	0.660	20.0	0.262
6.0	0.470	24.0	0.222
7.0	0.395	28.0	0.202
8.0	0.290	32.0	0.174
9.0	-	36.0	-
10.0	-	40.0	-

Table V

EXPLANATION OF PLATE VII

Fig. 5. Plot of distribution of the center line velocity  
for flow from a single jet. Outlet velocities

$$u_0 = 108 \text{ and } 270 \text{ fps.}$$

PLATE VII

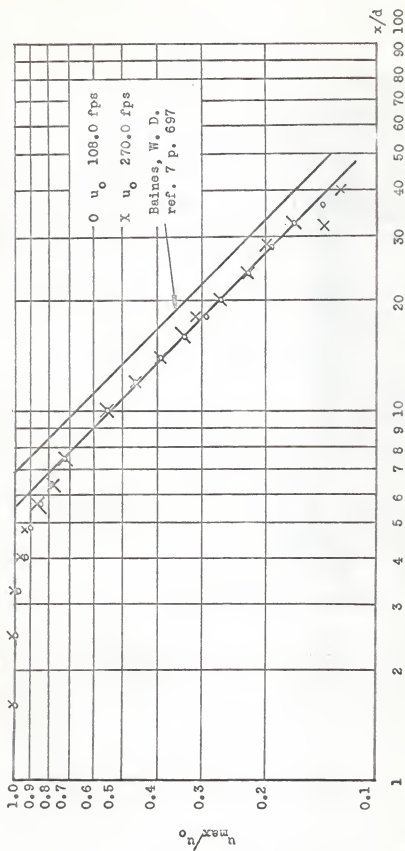


Fig. 5

EXPLANATION OF PLATE VIII

Fig. 6. Plot of distribution of the center line velocity  
for flow from a central hole( 3 holes spaced 1").  
Outlet velocities  $u_0 = 61.4, 109.0$  and  $212.0$  fps.

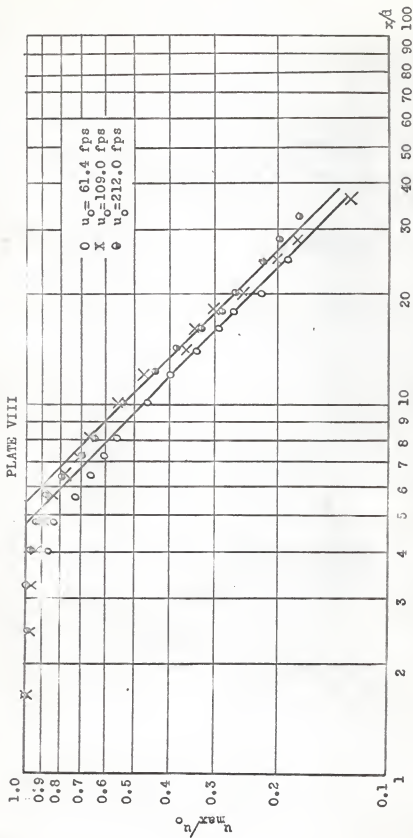


Fig. 6

EXPLANATION OF PLATE IX

Fig. 7. Photographic projection of the jets at 1 inch  
spacing and outlet velocity  $u_o = 33.4$  fps.

Equation for the breadth  $b_1 = 0.094x + 0.125$  (in).



## PLATE IX

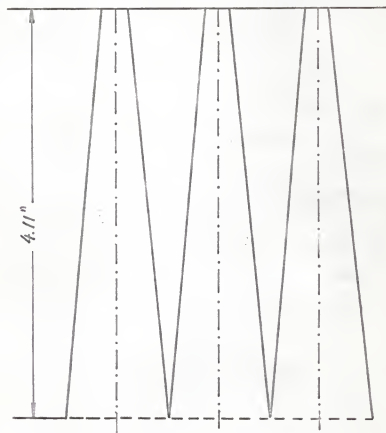


Fig. 7

EXPLANATION OF PLATE X

Fig. 8. Photographic projection of the jets at 1 inch spacing and outlet velocity  $u_0 = 48.4$  fps.

Equation for the breadth  $b_2 = 0.087x + 0.125(\text{in})$ .

## PLATE X

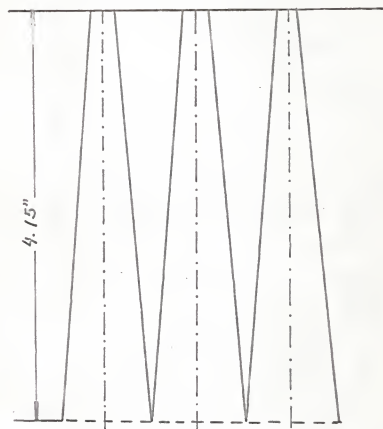


Fig. 8

EXPLANATION OF PLATE XI

Fig. 9. Photographic projection of the jets at 1 inch  
spacing and outlet velocity  $u_o = 63.0$  fps.  
Equation for the breadth  $b_3 = 0.093x + 0.125(\text{in})$

## PLATE XI

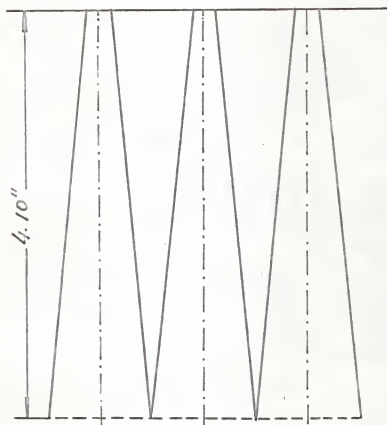


Fig. 9

EXPLANATION OF PLATE XII

Fig. 10. Photographic projection of the jets at 1 inch

spacing and outlet velocity  $u_o = 76.7$  fps.

Equation of the breadth  $b_4 = 0.087x + 0.125(\text{in})$ .

## PLATE XII

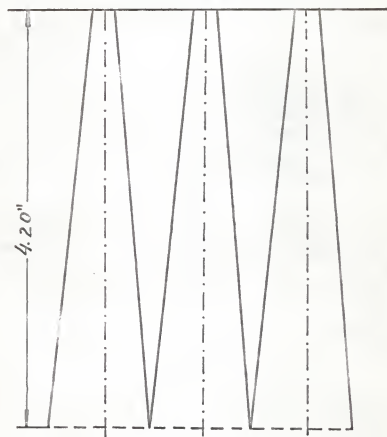


Fig. 10

EXPLANATION OF PLATE XIII

Fig. 11. Photographic projection of the jets at 1 inch spacing and outlet velocity  $u_0 = 91.6$  fps.

Equation for the breadth  $b_g = 0.076x + 0.125(\text{in})$ .



## PLATE XIII

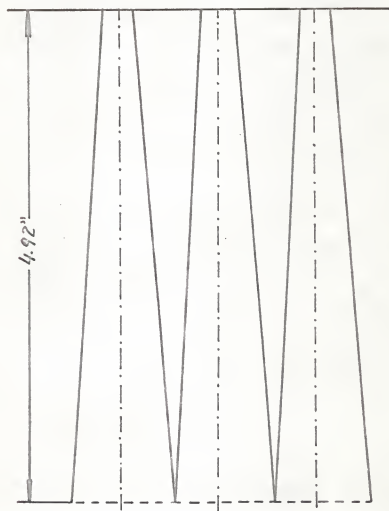


Fig. 11

EXPLANATION OF PLATE XIV

Fig. 12. Interaction of three jets at 1 inch spacing.

Outlet velocity  $u_o = 33.4$  fps and  $1/4$ " hole  
diameter.

## PLATE XIV



Fig. 12

EXPLANATION OF PLATE XV

Fig. 13. Interaction of three jets at 1 inch spacing.

Outlet velocity  $u_o = 49.4$  fps and  $1/4$ " hole  
diameter.

## PLATE XV



Fig. 13

EXPLANATION OF PLATE XVII

Fig. 14. Interaction of three jets at 1 inch spacing.

Outlet velocity  $u_o = 63.0$  fps and  $1/4"$  hole  
diameter.

## PLATE XVII



Fig. 14

EXPLANATION OF PLATE XVIII

Fig. 15. Interaction of three jets at 1 inch spacing.

Outlet velocity  $u_o = 76.7$  fps and  $1/4$ " hole  
diameter.



## PLATE XVIII



Fig. 15

EXPLANATION OF PLATE XIX

Fig. 16. Interaction of three jets at 1 inch spacing.

Outlet velocity  $u_0 = 91.6$  fps and  $1/4$ " hole  
diameter.

## PLATE XIX



Fig. 16

#### EXPLANATION OF PLATE XX

Table VI. Comparison of measured and predicted values of equalization velocity for a three jet pattern.

Table VII. Comparison of measured and predicted values of equalization velocity for a nine jet pattern.

## PLATE XX

$u_o$ (fps)	$x$ (in)	$\Delta EMF$ (mv)	$1/\Delta EMF$ (1/mv)	$u_{max}$ (fps)	
				measured	predicted
63.0	9.4	0.160	6.25	8.14	8.05
76.7	10.5	0.150	6.65	9.30	9.14
91.6	11.5	0.140	7.15	10.90	10.50

Table VI

$u_o$ (fps)	$x$ (in)	$u_l$ (fps)	$u_o$ (fps)	$u_r$ (fps)	$u_{max}$ (fps)
					predicted
63.0	9.4	8.03	8.10	8.03	8.05
76.7	10.5	9.05	9.12	9.05	9.14

Table VII

Note. The subscripts r, o and l refer to measurements at one inch on the right of the central hole, in the center of the central hole and at one inch on the left of the central hole, respectively.

EXPLANATION OF PLATE XXI

Fig. 17. Plot of equation  $b = ax + e$  for outlet velocities  
equal to 33.5, 48.5, 63.0, 76.7 and 91.6 fps

## PLATE XXI

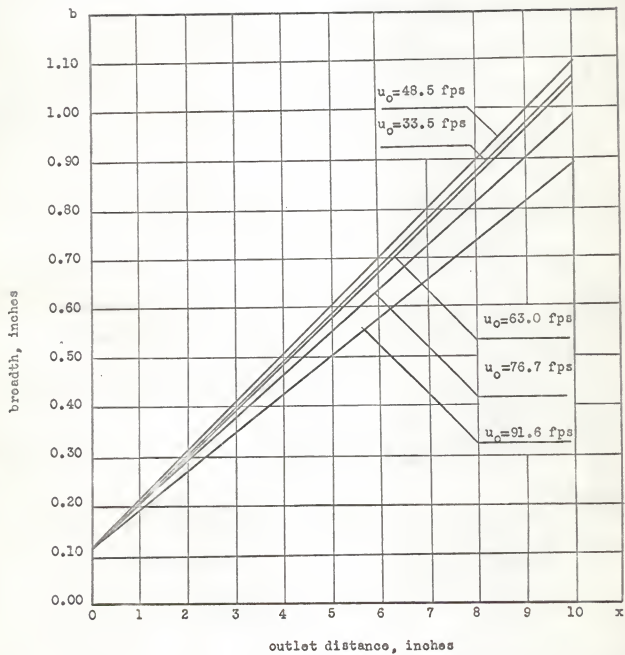


Fig. 17

INTERACTION OF VENTILATING JETS

by

ARNALDO MARANCONI

Engenheiro de Aeronautica-Aeronaves  
Brazilian Aeronautical Institute of  
Technology, 1963

---

AN ABSTRACT OF A  
MASTER THESIS

submitted in partial fulfillment of the  
requirements for the degree

MASTER OF SCIENCE

Department of Mechanical Engineering

KANSAS STATE UNIVERSITY  
MANHATTAN, KANSAS

1966



Jets issuing from 1/4 inch diameter holes were studied both experimentally and analytically. Some simplifying assumptions were made pertaining to the nature of the interacting jets. It was assumed therefore that the velocity profiles could be superimposed.

From Prandtl's mixing length theory an equation for the breadth was developed and the constants determined experimentally. From the momentum equation an expression was derived for the center line velocity distribution. The experimental results showed that the theoretical procedures adopted in order to determine the velocity of equalization is reasonable, although not extremely accurate. A suggested procedure is given for the theoretical determination of the velocity of equalization of interacting parallel jets.